**Calhoun: The NPS Institutional Archive**

**DSpace Repository**

Theses and Dissertations 1. Thesis and Dissertation Collection, all items

1968

# Deformation and fracture of a metal matrix composite model system.

Fusch, Kenneth Ericson

Massachusetts Institute of Technology

http://hdl.handle.net/10945/11924

*Downloaded from NPS Archive: Calhoun*

Calhoun is the Naval Postgraduate School's public access digital repository for research materials and institutional publications created by the NPS community. Calhoun is named for Professor of Mathematics Guy K. Calhoun, NPS's first appointed -- and published -- scholarly author.

Dudley Knox Library / Naval Postgraduate School
411 Dyer Road / 1 University Circle
Monterey, California USA 93943

http://www.nps.edu/library

NPS ARCHIVE
1968
FUSCH, K.

Master of Science

# DEFORMATION AND FRACTURE OF A METAL MATRIX COMPOSITE MODEL SYSTEM

BY

KENNETH ERICSON FUSCH

Course I June/1968

Thesis
F97

DUDLEY KNOX LIBRARY
NAVAL POSTGRADUATE SCHOOL
MONTEREY CA 93943-5101

# DEFORMATION AND FRACTURE OF A METAL MATRIX COMPOSITE MODEL SYSTEM

by

KENNETH ERICSON FUSCH
BS, United States Naval Academy
(1964)

Submitted in partial fulfillment
of the requirements for the degree of

Master of Science in Civil Engineering

at the
Massachusetts Institute of Technology

(June 1968)

IBRARY
AL PO [illegible] HOOL
[illegible] 93940

## ABSTRACT

# DEFORMATION AND FRACTURE OF A METAL MATRIX COMPOSITE MODEL SYSTEM

by

KENNETH ERICSON FUSCH

Submitted to the Department of Civil Engineering on 17 May 1968 in partial fulfillment of the requirements for the degree of Master of Science in Civil Engineering.

A continuous-fiber metal matrix composite model system is experimentally developed by combining large diameter (1/16") stainless steel fibers, or rods, with a matrix of high purity aluminum. The model system is designed to compare closely with actual composite systems in the following ways: (1) stress-strain behavior, (2) mode of failure, (3) theoretical predictions of strength, and (4) the development of fiber tensile stress through matrix shear stress transfer.

The critical aspect ratio for the model system is determined by using the pull-out load method. Both 3-fiber and 5-fiber models are fabricated by a gravity casting technique. Mechanical testing of specimens is carried out in tension parallel to the fiber axis.

Deformation of the pure aluminum matrix is studied through direct microhardness measurements of strain hardening. Qualitative analysis of the stress-strain behavior and the fracture mode is also made.

Results show that the model systems exceed rule-of-mixtures strength predictions, thereby indicating that synergistic effects are present. Microhardness test results verify the existence of high levels of matrix shear stress near the fiber ends.

Thesis Supervisor: Russel C. Jones, Ph.D.

Title: Associate Professor of Civil Engineering

# ACKNOWLEDGMENTS

The author wishes to express his sincere appreciation to Professor Russel C. Jones for his invaluable advice and constant direction throughout the duration of the research for and the preparation of this thesis.

The help and suggestions of fellow students Elliot F. Olster and Donald Scarlett have been most beneficial and are greatly appreciated.

The author is grateful to Mr. Arthur P. Rudolph for his guidance in the preparation of test specimens and to Mr. Laszlo Szekessy for his assistance with many aspects of the experimental work.

Special thanks are due my wife Betty for her patience, understanding, and encouragement.

## TABLE OF CONTENTS

Page:

Title Page.................................... 1

Abstract...................................... 2

Acknowledgments............................... 3

Table of Contents............................. 4

Body of Text.................................. 5

I. Introduction............................... 5

- General.................................... 5
- Use of Model Systems....................... 7

II. Model Systems Design...................... 12

- The Pull-Out Load Method................... 12
- Development of Model Design................ 16

III. Fabrication of Model Systems............. 19

- Selection of Materials..................... 19
- Model Fabrication.......................... 22
- Effects of Fabrication on Fiber Properties.................................. 25

IV. Deformation and Fracture.................. 28

- Stress-Strain Behavior..................... 28
- Matrix Deformation......................... 29
- Composite Fracture......................... 33

V. Conclusions................................ 38

References.................................... 40

Figures....................................... 43

Appendix...................................... 64

List of Figures............................... 65

# I. INTRODUCTION

## General

The development of filamentary materials with extremely high strengths and stiffnesses has given impetus to the growth of the field of composite materials. Strong fibers have been successfully combined with matrix materials of a dissimilar nature to produce new products with superior mechanical properties.

The use of a metallic matrix gives many advantages over non-metallic matrices, among these being improved high-temperature performance. The plastic flow characteristics of a metal matrix provide a means for efficient stress transfer between fibers and a reduction in the notch-sensitivity of the composite [1]*. The ability of a metal matrix to strain harden introduces still another improvement in overall composite performance. Lightweight metallic matrices have the added benefit of allowing fabrication of fibrous composites with high specific strengths and stiffnesses.

Metal matrix composites hold great potential for future engineering applications. The aerospace industry which places a premium on high strength/lightweight

---

* Numbers in brackets refer to references listed at the end of this report.

materials has been first to capitalize on the early development of fiber-reinforced metals.

Current research is being conducted on two fronts: (1) the improvement of fabrication techniques, coupled with an attempt to understand more fully how fabrication variables affect the final product, and (2) a better understanding of the mechanics, both micro- and macro-, of composite behavior. Two drawbacks are apparent at this stage of composite development. The anisotropic nature of fibrous composites places limitations on structural applications, and the high cost of these materials places the product out of economic reach for many applications. Current high costs, however, are due primarily to the initial research and development efforts, and significant price reductions can be anticipated in the future.

The earlier development of fiber-reinforced plastics has provided a bonus for investigators in the field of metal matrix composites. Many techniques of experimental research used in fiber-reinforced plastics, as well as much of the basic theoretical work, can be utilized in the expanding metal matrix composite research effort. However, the markedly different characteristics of metallic and non-metallic matrices have called for some modifications to the theoretical picture and for new experimental approaches. Much work in fiber-reinforced plastics has involved the use

of birefringent resin matrices to study the principles of composite action - a technique which obviously cannot be carried over to metal matrix composites. New approaches have been devised, however, and many more are in the planning stages. A successful approach to studying the plastic deformation characteristics of ductile metallic matrices has involved the measurement of matrix strain hardening through the use of direct microhardness techniques.

## Use of Model Systems

Sutton [2] has classified studies on fiber-reinforced metals into the following two categories: "(1) those dealing with the careful preparation of model composite systems to modify or extend existing theories, and (2) those dealing with various metals and alloys reinforced with both metallic and ceramic fibers to develop useful engineering materials." In the latter category, numerous investigators [3,4,5] have published papers discussing the fabrication and performance of specific metal matrix composite systems. Although these research efforts are not elaborated upon herein, it is important to note that the aluminum/stainless steel composite discussed by Davis [6] serves as a reference point for the model system developed and studied in this research effort.

The use of metal matrix composite model systems has provided the basis for much of the presently accepted theory on composite strength and behavior. Model systems have been used extensively because (1) better control over fabrication variables can be maintained and (2) more success in isolating, or separating, experimental parameters can be achieved. Such problems as fiber alignment, interfiber spacing and eccentricity of loading can be minimized or overcome through model techniques. Stress concentrations due to various fiber end geometries in discontinuous-fiber composites can be handled more effectively through the use of single-fiber model systems. The effects of metallurgical reactions between fiber and matrix resulting from various fabrication processes can be studied in greater detail through model systems. Burte et al [7] have studied the various interactions that can occur during composite fabrication and/or subsequent elevated temperature exposure with model systems in which the metals used for fiber and matrix were selected on the basis of metallurgical considerations, rather than ultimate mechanical performance.

Another approach with model systems involves the study of the micromechanics of fibrous composite behavior. Experimental work by Ebert et al [8] has employed model systems of both densely-packed and loosely-packed multifilament composites to develop design criteria for composite

materials. The work of Ebert considers such problems as the effects of residual stresses due to differences in coefficients of thermal expansion and the occurrence of a triaxial stress state in both fiber and matrix during uniaxial loading.

Many composite model systems which have been studied to date have been fabricated with materials that have been selected for reasons of experimental convenience. Material combinations which have minimal chemical reactions, compatible coefficients of thermal expansion, or good surface wetting characteristics have often been chosen. The result has been the development of model systems which are non-practical composites. Although these model systems have been beneficial in formulating basic composite theory, their usefulness in solving practical problems is often limited. The materials used in this model study have been chosen in an attempt to circumvent this limitation. It is anticipated that the carry-over from model system performance to actual composite development will be enhanced through the use of an aluminum/stainless steel system.

The use of an array of large diameter fibers in a metallic matrix represents a new approach to modeling techniques. The use of small-scale models is not new; structural engineers have used this method for years to gain insight into the performance of actual structures. However, the

use of large-scale models in materials science is a relatively new concept. Ebert's work involves just such an approach. It is expected that a better understanding of the macromechanics of scaled-up models will shed significant light on the micromechanics of actual composite systems.

The metal matrix composite model system of this research effort is a large diameter, continuous-fiber system. Continuous fibers, with a diameter roughly one order of magnitude larger than the diameter of many commercially available fibers used in composite fabrication, are used in conjunction with an extremely ductile matrix, high purity aluminum. Although the strength properties of the large diameter fibers, or rods, are much lower than the corresponding values for typical metallic fibers found in practical composites, the use of low strength pure aluminum as the matrix maintains good correlation between fiber properties and matrix properties.

The object of this work has been twofold: (1) to develop a useful continuous-fiber metal matrix composite model system and (2) to study the deformation and fracture characteristics of such a model system. The validity of the model system is based on the following criteria:

(1) stress-strain behavior
(2) mode of failure
(3) theoretical predictions of strength
(4) the development of fiber tensile stress through matrix shear stress transfer

To be a valid model, the system developed must compare closely with actual composite systems in each of these categories.

# II. MODEL SYSTEM DESIGN

## The Pull-Out Load Method

In order to ensure proper composite behavior in the continuous-fiber model systems, it was necessary to determine the critical length of fibrous reinforcement, i.e., the minimum length of fiber which must be embedded in the matrix. Only when the length of fibrous reinforcement equals or exceeds this critical length will there be sufficient fiber-matrix interfacial area to cause fiber fracture through the mechanism of shear stress transfer. Weeton and Signorelli [9] discuss the process of fiber-matrix load transfer for both continuous and discontinuous fibers. The critical length, $L_c$, has been shown to be a function of fiber diameter, D; the ultimate tensile strength of the fiber, $\delta_f$; and the shear strength of the interfacial bond or the shear strength of the matrix, $\tau$, whichever is less. This relationship, in terms of the critical aspect ratio, $\frac{L_c}{D}$, is given by

$$\frac{L_c}{D} = \frac{1}{4}\frac{\delta_f}{\tau} \qquad \text{(Eq. 1)}$$

This expression serves as the basis of an experimental method of determining the critical aspect ratio. This

method is the single-fiber pull-out load test. There are certain drawbacks, however, to the use of the pull-out test. Since only a portion of the fiber is embedded in the matrix, tensile load is applied directly to the fiber rather than through interfacial shear stresses along the entire fiber axis as would be the case in an actual composite [10]. In addition, the use of a single fiber does not take into account the influence of surrounding fibers [11]. Regardless of these limitations, the method has been used by numerous investigators and it appears to be sound at least qualitatively.

The pull-out test is based upon the concept that fibers embedded in a matrix material to depths less than half the critical length, $\frac{L_c}{2}$, will pull-out, whereas fibers embedded to depths greater than $\frac{L_c}{2}$ will fracture. Thus, the critical length is established as twice the depth at which pull-out ceases to be the mode of failure and fiber fracture begins. The use of equation (1) will give an indication of the degree of bonding between fiber and matrix. However, this relationship cannot be used to obtain precise values of interfacial or matrix shear strength due to the nonuniformity of the shear stress distribution along the fiber axis. It is more realistic to assume that the value of $\tau$ obtained from equation (1) is an average interfacial shear stress. The nonuniformity of the interfacial shear

stress is shown more clearly in Figure 1, which is a schematic representation of the shear stress distribution along the fiber axis for various lengths of fiber embedded in the matrix. The build-up of fiber tensile stress is also plotted. The assumption of a linear tensile stress build-up along the fiber is supported by Kelly and Davies [12].

Stainless steel fibers ($\frac{1}{16}$" diameter) were embedded in pure aluminum at various depths ranging from $\frac{5}{8}$" to almost 4". Pull-out tests were conducted on an Instron testing machine at a crosshead rate of 0.1 inches per minute. Blunted end fibers were used in all pull-out specimens. Figure 2 shows a sample pull-out specimen prior to testing. Gripping of specimens in the Instron testing machine was done in such a manner that no lateral restaint was exerted upon the fiber during testing. Shown in Figure 3 is a plot of failure load (maximum pull-out load) vs. length/diameter ratio for stainless steel fibers in pure aluminum.

It is apparent from the data in Figure 3 that the results of the pull-out tests can be used to establish the critical aspect ratio. A definite change in failure mode was observed at a length/diameter ratio of 36. It is also apparent that the results for the test specimens that failed by fiber pull-out (less than half the critical length embedded) do not agree with the theoretical expectations as shown by the dashed line. This theoretical curve is based

upon the assumption of a uniform interfacial shear stress distribution along the fiber axis. It further assumes that the blunted end fiber is unbonded to the matrix. The data suggest a parabolic, rather than linear, relationship in this region. This behavior can be explained by (1) matrix strain hardening and (2) high interfacial or matrix shear stresses near the fiber ends.

The stress-strain behavior of the high purity aluminum matrix is such that plastic flow occurs at low levels of stress. Associated with this plastic flow is strain hardening. As tensile load is applied to the fiber during the pull-out test, plastic flow takes place in the matrix in the vicinity of the fiber. This transfer of stress is brought about by the interfacial bonding between fiber and matrix. As the matrix flows, strain hardening produces an increase in the resistance to fiber pull-out. This caused a higher maximum pull-out load than would have been recorded if no matrix strain hardening occurred. Evidence to support this has been obtained through direct microhardness techniques. An increase in Vicker's Hardness Number from 20.7 to 22.9 was found in the pure aluminum matrix adjacent to the fiber cavity after pull-out testing. This increase was not as large at distances of $\frac{1}{2}$ fiber diameter and 1 fiber diameter away from the cavity.

The fiber-matrix interaction has been shown to manifest itself in high values of shear stress near fiber ends

[13,14]. These high shear stresses are present even when the fiber length is less than critical; hence, the resistance to fiber pull-out is greater than would be anticipated if the interfacial or matrix shear stresses were constant along the fiber axis. (Refer to Figure 1).

An additional reason for the high pull-out loads (for the case where less than half the critical length is embedded) is bonding at the fiber ends. Although this is probably a minor cause for the high loads, it is interesting that Kelly and Tyson [15] have noted that "there is an appreciable stress transferred across the fiber end for specimens with the end bonded to the matrix."

## Development of Model Design

The final design of the continuous-fiber metal matrix composite system was based upon the experimental determination of the critical aspect ratio and upon a method of tensile loading that (1) would assure proper composite stress-strain behavior and that (2) would develop the ultimate tensile strength of the fibers through the transmission of shear stress through the matrix, rather than through any direct tensile stress on the fibers. A circular cross-section was ultimately selected to aid in model fabrication during machining operations. Design of the circular cross-section for the 3-fiber and the 5-fiber models used in this

study is shown in Figure 4.

Initial plans for conducting tensile tests of the continuous-fiber models called for the ends of the test specimens to be held with conventional grips which exert lateral restraining forces on the specimen ends, as shown schematically in Figure 5A. Two reasons can be cited as justification for abandoning such conventional grips for shoulder grips: (1) the extreme ductility of the pure aluminum matrix and (2) the desire to introduce tensile stresses in the fibers solely through the action of shear stress transfer through the matrix, rather than through artificial means. At this stage, design of the model system was modified as shown in Figure 5B. (Note the arrows which indicate the nature of the tensile loading). The specimen length between points of load application was set at $L_c$ to guarantee that adequate tensile stress would be built up within the fibers to cause fracture. Several 3-fiber models were fabricated according to this design. Subsequent tensile testing revealed that this modified design did not work properly, i.e., the mode of failure was a matrix shear failure with no fiber fracture occurring. Photographs of the failure mode of several of these improperly designed specimens are shown in Figure 6.

A further modification in model design was introduced at this point. The alteration involved a change in the

points of load application such that one-half of the critical length was outside of the loading points as illustrated in Figure 5C. This final modification worked satisfactorily and both the 3-fiber and 5-fiber models were designed accordingly. Figure 7 shows the final model system design prior to testing and after fracture.

## III. FABRICATION OF MODEL SYSTEMS

### Selection of Materials

The model systems used in this research effort have been composed of 1/16" diameter stainless steel fibers in a matrix of pure aluminum. The choice of stainless steel and aluminum for the fibers and matrix, respectively, was based upon two reasons: (1) stainless steel/aluminum composites are currently available commercially; hence a good reference exists for making comparisons between actual metal matrix composite behavior and the model system behavior; (2) low cost and availability of materials. The steps used in fabricating a commercial 2024 aluminum/NS355 stainless steel (.009 inch diameter fibers) composite are described in detail by Sumner [16].

The aluminum used as the matrix had a purity of 99.99%. The use of this high purity aluminum was desirable because of its high ductility, low strength, and good strain hardening characteristics. Mechanical testing revealed an ultimate tensile strength of 6600 psi., a yield strength (0.2% offset) of 2900 psi. and an elongation in 2" of 50%. These values agree closely with published mechanical properties for this grade of high purity aluminum [17].

The selection of aluminum as the matrix metal seemed warranted in view of its high potential usefulness as a matrix

in future commercial applications. Such characteristics as no ductile-brittle transition and low load-rate sensitivity, coupled with its light weight and low cost, make aluminum and its alloys very attractive as metallic matrices.

AISI type 304 stainless steel in 1/16" diameter rods (fibers) was selected for use in this experimental work. Type 304 is an austenitic stainless steel with the following approximate chemical composition [18]: 18-20% Cr, 8.0-12.0% Ni, 0.08% C, 1.0% Si, 2.0% Mn, 0.045% P, and 0.03% S. Typical mechanical properties include an ultimate tensile strength of 127,000 psi., a yield strength (0.2% offset) of 93,000 psi., and an elongation of 2" of 47%. The choice of an austenitic stainless steel over a martensitic stainless steel was based upon a higher elongation in the former. The use of a ferritic stainless steel did not seem desirable due to the possibility of 885°F embrittlement during the high temperature fabrication procedure used in this work.

The use of extremely ductile fibers is actually a limitation of the model system, although it is an experimental necessity. The high strength fibers used in most metal matrix composites are relatively brittle. The high degree of ductility (measured by fiber elongation) was necessary to ensure that the fiber volume fraction in the continuous-fiber model systems would exceed both the minimum volume fraction and the critical volume fraction which are

defined by Broutman and Krock [19] in the following manner:

$$V_{f_{crit.}} = \frac{\delta_{mu} - (\delta_m)_{\varepsilon'_f}}{\delta^*_{fu} - (\delta_m)_{\varepsilon'_f}} \quad \text{(Eq. 2)}$$

$$V_{f_{min.}} = \frac{\delta_{mu} - (\delta_m)_{\varepsilon'_f}}{\delta^*_{fu} + \delta_{mu} - (\delta_m)_{\varepsilon'_f}} \quad \text{(Eq. 3)}$$

where, $\delta_{mu}$ = ultimate tensile strength of the metallic matrix,

$\delta^*_{fu}$ = ultimate tensile strength of the fibers,

$(\delta_m)_{\varepsilon'_f}$ = matrix stress when the fibers are strained to their ultimate tensile strain.

The volume fraction of fibers, $V_f$ , in a metal matrix composite must exceed $V_{f_{crit.}}$ if fiber strengthening is to occur, i.e., if the ultimate tensile strength of the composite, $\delta_{cu}$ , is to exceed the strength of the strain hardened matrix alone. $V_f$ must exceed $V_{f_{min.}}$ if the strength of the composite is to be found from the following rule-of-mixtures relationship:

$$\delta_{cu} = \delta^*_{fu} V_f + (\delta_m)_{\varepsilon'_f}(1 - V_f) \quad \text{(Eq. 4)}$$

The use of high ductility stainless steel fibers in the model systems results in low values of $V_{f_{min.}}$ and $V_{f_{crit.}}$. Because the ultimate tensile strain of the fibers is very high, the stress in the matrix at the point of fiber fracture is only slightly less than the ultimate tensile stress of the matrix. Thus the numerators of both equations (2) and (3) are quite small, giving rise to negligible values of $V_{f_{min.}}$ and $V_{f_{crit.}}$

The limitation imposed by the use of very ductile fibers does not reduce the validity of the model system significantly since the fibers in some commercial composites fracture in a ductile fashion. The scanning electron micrograph shown in Figure 22 clearly shows a classical cup-and-cone fracture mode for the fibrous reinforcement. To circumvent this ductile fiber limitation, a martensitic stainless steel such as AISI type 416 (with a fiber elongation of only 10-30%) might be employed in a similar model design. However, this would require that the model system volume fraction be somewhat higher in order to exceed $V_{f_{min.}}$ and $V_{f_{crit.}}$.

Model Fabrication

Both the continuous-fiber models and the pull-out test specimens were fabricated by using a gravity casting technique. This technique involved pouring molten aluminum into a graphite mold which [illegible] stainless steel fibers.

The two graphite mold designs used for casting were as follows: (1) a vertical circular mold for continuous-fiber models and (2) a horizontal rectangular mold for the pull-out test specimens. The molds are pictured in Figure 8. Grade CS graphite was used for both molds.

All castings were done in an air environment with the molds and the stainless steel fibers at room temperature prior to the introduction of the molten aluminum into the molds. Pure aluminum in ingot form was placed in a crucible and then heated to its melting point (660°C) in a laboratory furnace. The molten aluminum was next heated to a temperature of 1000°C before pouring. The reasons for this additional heating above the melting point were (1) to ensure molten aluminum flow around the fibers in the model systems before solidification began and (2) to improve the quality of the fiber-matrix bonding by promoting some metallurgical interaction.

Preliminary investigations revealed that some surface preparation of the 1/16" stainless steel fibers was necessary to ensure an acceptable degree of bonding during fabrication. Accordingly, the following three-step fiber cleaning operation was employed to aid in the removal of oxide layers, oil and grease films, and other unwanted debris:

(1) rubbing with emery cloth
(2) 1 minute agitation in methanol (methyl alcohol)
(3) 1 minute agitation in petroleum ether (benzine)

Upon completion of fiber cleaning, the stainless steel fibers were arranged in the appropriate graphite mold and the 1000°C molten aluminum was poured into the mold. The molten aluminum was then allowed to solidify and to continue cooling in air until the model system casting reached room temperature. This relatively slow cooling of the model system was permitted so as to take advantage of solid state diffusion which occurs at high temperatures in an attempt to improve fiber-matrix bonding. Slow cooling also assured a large grain size in the matrix as can be seen in Figure 9. This large grain size was necessary so that the mean grain diameter would be on the same order of magnitude as the fiber diameter and hence increase the validity of the model system. This relationship between approximate matrix grain size and fiber diameter is found in many commercial composites such as the aluminum/stainless steel composite used as a reference point.

After the model composites reached room temperature, they were removed from the graphite molds in preparation for machining. Figure 10 shows a continuous-fiber model and a pull-out test specimen in the as-cast condition. All model systems and pull-out specimens were machined into the appropriate shapes for mechanical testing through the use of a conventional lathe and a horizontal milling machine. Figure 11 is a scaled drawing of both a pull-out test specimen and

a continuous-fiber model.

## Effects of Fabrication on Fiber Properties

The fabrication of metal matrix composites often involves processes that alter the mechanical properties of the fibrous reinforcement. This alteration of fiber properties may or may not enhance the performance of the composite. Sutton [2] discusses this problem, pointing out that considerable care must be exercised during all stages of fabrication to ensure that fibers are not damaged or weakened. Brittle fibers such as boron and silica are quite susceptible to fracture during such operations as cold rolling or hot pressing. Ductile fibers are less prone to fracture during these operations; however all fibrous reinforcement is subject to degradation through combinations of chemical reaction and/or diffusion. Exposure to high temperature environments can change the mechanical properties of metallic fibers through the process of annealing or by various types of embrittlement.

The method used in fabricating the continuous-fiber aluminum/stainless steel model systems discussed herein involves the casting of molten aluminum around stainless steel fibers, thereby subjecting the fibers to a high-temperature environment for a substantial period of time. To gain some insight as to how the fiber properties are affected by this

high-temperature environment, a plot of fiber temperature vs. time in the fabrication process was determined as shown in Figure 12. To obtain accurate data for this plot, a chromel-alumel thermocouple was placed in the center of a graphite mold. This was accomplished by sliding the thermocouple wires into two small holes in a 1/8" hole in the end of the graphite mold in such a manner that the chromel-alumel junction occupied a position at the center of the mold. Molten aluminum heated to 1000°C was poured into the mold and allowed to solidify and cool around the thermocouple. Temperature readings were taken at specified intervals of time.

The primary concern with type 304 stainless steel was a possible change in its mechanical properties through the process of annealing. Austenitic stainless steels are annealed at temperatures between 950°C and 1100°C [18]. Since the fiber temperatures dropped below this annealing range almost immediately, it is assumed that negligible change in the fiber mechanical properties took place. To further substantiate this assumption, type 304 stainless steel fibers were heated for 30 minutes at temperatures ranging from 800°C to 1000°C. The results of mechanical testing of these specimens indicated that an average ultimate strength reduction of only 12% occurred due to this excessive heating. Fiber elongation did not increase appreciably until the temperature reached 1000°C for the 30 minute period.

Optical microscopy indicated that there was no formation of an interfacial third phase around the fibrous reinforcement as a result of the elevated temperature fabrication process.

# IV. DEFORMATION AND FRACTURE

## Stress-Strain Behavior

In order to study the deformation and fracture characteristics of the large fiber metal matrix composite model system, the 3-fiber and 5-fiber models were subjected to tensile loading parallel to the fiber axis. Loading was carried out through the use of an Instron testing machine at a crosshead rate of 0.1 inches per minute. It is important to recall that the manner of loading developed herein applies no direct tensile stresses to the fibers; fiber tensile stress is generated indirectly through the mechanism of shear stress transfer through the matrix.

Kelly and Davies [12] postulate that the stress-strain behavior of metal matrix composites can be divided into the following four stages:

Stage I. Elastic deformation of both fiber and matrix
Stage II. Fiber elastic, but matrix now plastic
Stage III. Plastic deformation of both fiber and matrix
Stage IV. Fiber fracture followed by matrix failure

This four-stage behavior is supported by the performance under tensile stress of both tungsten fiber-copper matrix composites and stainless steel fiber-aluminum matrix composites. Figure 13 shows the four stages of composite deforma-

tion schematically. A theoretical analysis of ideal fiber-reinforced composites by MacFadyen and Jones [20] agrees with this stress-strain behavior.

Practical considerations arising with the type of loading used for the 3-fiber and 5-fiber models prohibited an accurate measurement of strain during the loading process. Figure 14 shows one end of a model system in a shoulder grip. Hence, the determination of a stress-strain curve for the models was not possible. Load-deformation curves for the model systems are shown in Figures 15 and 16. These curves indicate that four-stage composite behavior does occur for both model systems. The end of stage III deformation for fiber-reinforced composites is marked by fracture of the high-strength fibers. This point is shown distinctly on the load-deformation curves. Stage I terminates when the matrix ceases to behave elastically. This point is also revealed in Figures 15 and 16. The transition from stage II to stage III is less pronounced, however this is characteristic of fibrous composites reinforced with ductile fibers.

## Matrix Deformation

The strain hardening characteristics of the metallic matrix play an important role in the overall performance of a

tion successfully. A theoretical analysis
modified compactly by Hurlstein and
with this stress-strain behavior.

Practical considerations arising from
loading used for the 3-fiber and 5-fiber
an accurate measurement of its linearity
Figure 15 shows the
Hence, the deterioration of
models was not possible adequate
model systems are shown
indicate that
both model systems
fiber-reinforced
strength
deformation
tested in
in Figure
III to
(Tables

Table

Fiber
matrix

metal matrix composite. Plastic flow of the metal matrix serves as the primary means of shear stress transfer in fibrous composites and it can produce considerable strain hardening. The elastic-plastic transition in high purity aluminum occurs at very low levels of stress, hence strain hardening begins early in the stress-strain life of composites fabricated with pure aluminum matrices. A technique for studying the plastic deformation of metallic matrices, and thus the level of stress, has been used by Jones [21]. This technique involves the determination of the amount of strain hardening by direct microhardness measurements. This method has been used by Parikh [13] to verify the existence of high levels of stress near fiber ends by experimentation with a single short tungsten fiber in a silver matrix.

The experimental procedure used involved the determination of the Vicker's Hardness Number for various key locations in the model systems. As reference points for microhardness testing, the Vicker's Hardness Number was obtained for uncomposited pure aluminum in both an unstressed condition and after tensile failure. The average $H_V$ for the unstressed aluminum was 20.7; the average $H_V$ for the aluminum loaded in tension until fracture was 30.4. These two values of $H_V$ represent the lower and upper bounds of microhardness for pure aluminum. Thus, a 50% increase in microhardness can be realized in pure aluminum in going from an unstressed to a

fractured condition.

After mechanical testing of the model systems had been completed, the test specimens were sectioned in such a manner as to expose various critical areas in which microhardness readings were to be taken. Sectioning of specimens was accomplished by a spark erosion cutting process so as to minimize any additional plastic deformation of the exposed surfaces as would occur with standard mechanical cutting procedures. All cutting was done with a Servomet spark cutter using the finest cutting rate available (no. 7). Specimen surfaces were then electropolished with a perchloric acid solution to remove any surface deformation caused by spark cutting and to produce a relatively smooth surface for making microhardness indentations.

A Leitz microhardness tester was employed to make microhardness indentations. The Vicker's Hardness Number at designated locations was determined by making a series of four diamond indentations as shown in Figure 17. The average value of $H_V$ for the cluster of four indentations thus gives an indication of the amount of strain hardening in the aluminum matrix at areas of interest. Figure 18 shows the areas on a longitudinal section where microhardness readings were taken. Readings were taken at each of the following radial distances from the fibers:

(1) Immediately adjacent to fiber - both within the fiber cage (interior) and

outside (exterior)

(2) 1/2 fiber diameter away

(3) 1 fiber diameter away

The results of the microhardness testing are shown in Figure 19 in which $H_v$ is plotted against fiber length. Values plotted are for readings taken adjacent to the fiber on both interior and exterior sides. The high values of $H_v$ in locations 1 and 2 can be explained on the basis of proximity to the point of final matrix failure. A decrease in hardness in locations 3 and 4 seems consistent in view of increasing distance from the point of matrix failure. An increase in hardness was found in locations 5 and 6. This evidence of large amounts of plastic deformation agrees well with the high level of matrix shear stress in this area necessary to generate sufficient tensile stress in the fiber to cause fracture. (Refer to Figure 1). Although the hardness values in Figure 19 are slightly higher for the interior case than for the exterior case, both curves exhibit the same general behavior. The discrepancy in hardness values is within the experimental error associated with microhardness testing. Values of $H_v$ in the matrix as a function of radial distance from the fiber are relatively constant. This finding substantiates the work of Jones [21] in which he reported that the shear stress transfer in the matrix does not involve appreciably higher strains in the immediate vicinity of the fibers.

To obtain more information about the matrix strain hardening characteristics at various critical locations on the cross-section, both the 3-fiber and 5-fiber models were sectioned perpendicular to the fiber axis approximately half the distance between the point of load application and the fracture surface. A high degree of hardness, indicating substantial plastic deformation, was found across both cross-sections. The only significant trend was somewhat higher values of $H_V$ in the vicinity of the fibrous reinforcement. This trend can be explained by a greater resistance to local plastic flow during the indentation process due to the close proximity of the fiber. No conclusive evidence of a triaxial stress condition or of a high residual stress level was detected in either cross-section. It appears that massive plastic deformation (during stage III) in the region between points of load application has obscured any meaningful data in this area. This excessive plastic deformation can be attributed to extreme fiber ductility. It is suggested that in future studies termination of tensile stress after completion of stage II deformation would allow more meaningful data to be obtained in this cross-sectional area.

## Composite Fracture

The principles of composite action require that sufficient tensile stress be developed in the fibrous reinforcement

to cause fracture. This requirement must be satisfied if the metal matrix composite is to reach its full strength potential. A secondary requirement is that fiber fracture should occur prior to failure of the metallic matrix. This condition brings about two benefits: (1) as fibers begin to fracture, segments of broken fiber still retain their bond with the matrix, acting as short discontinuous reinforcement, and (2) after all fibers fracture, the ductile metal matrix is still able to carry some proportionate part of the load, hence preventing immediate catastrophic failure of the composite. The 3-fiber model system and the 5-fiber model system developed in this study adhere to the two principles discussed above. This is supported by the load-deformation curves shown in Figures 15 and 16. As mentioned previously, the aluminum/stainless steel composite fabricated by the Harvey Engineering Laboratories of Torrance, California served as the basis for much of the development of these model systems. It is therefore interesting to compare a fracture surface micrograph of the Harvey composite with similar micrographs of the model systems. These micrographs are shown in Figures 20 - 22.

Of primary importance in the development of metal matrix composites are the high values of ultimate tensile strength which can be achieved. Composite performance can be evaluated on the basis of rule-of-mixtures predictions of ultimate

tensile strength. Kelly [22] states that such predictions are actually a theoretical lower limit for continuous-fiber composites. This can be justified on the basis of a triaxial state of stress in the matrix. The higher modulus fibers will exert a restraining effect on the matrix under uniaxial load, thereby creating triaxial stresses. The result will be a decrease in matrix deformation and a corresponding increase in the yield strength, ultimate strength, and modulus of the matrix [7]. Furthermore, synergistic behavior is common in the case of ductile fiber composites where fiber-matrix bonding serves as a deterent to localized plastic instability, or "necking".

The measured ultimate tensile strengths for the model systems were as follows: 12,350 psi. for the 3-fiber model and 15,100 psi. for the 5-fiber model. Predicted ultimate strength values were determined from the relationship given by equation (4) which gives ultimate strength values of 11,300 psi. for the 3-fiber model and 14,400 psi. for the 5-fiber model. It should be noted that for the purpose of rule-of-mixtures predictions that the matrix stress when the fibers are strained to their ultimate tensile strain is assumed to equal the ultimate tensile strength of the matrix, $(\delta_m)_{\varepsilon'_f} \simeq \delta_{mu}$. This assumption appears valid since the ductile stainless steel fibers exhibit such a large amount of elongation prior to fracture. Thus, it can be seen that actual

model system strengths exceed predicted rule-of-mixtures strengths be approximately 9% and 5% for the 3-fiber model and the 5-fiber model, respectively. It is apparent that synergistic effects are present in both model systems.

An analysis of the effects of both matrix strain hardening and triaxiality can be made if true stress, rather than engineering stress, values are used at the ultimate strength condition for the model systems. This approach is necessitated since a substantial reduction in area occurs in the model systems prior to the end of stage III deformation. Using an estimate of the actual composite cross-sectional area at the point of fiber fracture, the following data can be produced:

| 3-FIBER MODEL: | End of Stage I Deformation | Ultimate Strength Condition Based on True Stress |
|---|---|---|
| Composite Stress | 6,725 psi. | 16,300 psi. |
| Fiber Stress | 18,700* | 127,000 |
| Matrix Stress | 6,225* | 11,800 |

| 5-FIBER MODEL: | End of Stage I Deformation | Ultimate Strength Condition Based on True Stress |
|---|---|---|
| Composite Stress | 8,400 psi. | 19,900 psi. |
| Fiber Stress | 22,300* | 127,000 |
| Matrix Stress | 7,450* | 12,450 |

* Determined by ratio of elastic moduli [21].

The above data show a significant increase in the matrix stress level at the end of stage I deformation. Values of 6,225 psi. and 7,450 psi. for the 3-fiber and 5-fiber models, respectively, are considerably above the 2,900 psi. yield stress that would be expected at this point. This is indicative of substantial triaxiality in the model systems. The ultimate matrix stress levels for the models are both higher than the uncomposited U.T.S. of 8,750 psi. (true stress) for high purity aluminum. This is further evidence of triaxial stress conditions. The large increase in matrix stress in going from the end of stage I to fracture not only confirms triaxiality but also shows the effects of considerable matrix strain hardening. It should be noted also that the matrix stress for the 5-fiber model is higher than for the 3-fiber model both at the end of stage I and at ultimate strength conditions. This can be attributed to greater triaxial restraint in the 5-fiber model.

## V. CONCLUSIONS

The objectives of this research program in the field of metal matrix composites have been met. A continuous-fiber model system has been developed by combining large diameter stainless steel fibers, or rods, with a matrix of high purity aluminum. The 3-fiber and 5-fiber models meet the following four criteria for a valid model system: (1) a stress-strain behavior which compares closely with actual metal matrix composite systems, (2) a mode of failure which is the same as ideal composite failure, i.e., fiber fracture followed by matrix failure, (3) favorable comparison with rule-of-mixtures strength predictions, and (4) the generation of fiber tensile stress through the mechanism of matrix shear stress transfer rather than through any direct axial stress on the fibers.

The validity of the large fiber model system has been substantiated through qualitative studies of the stress-strain behavior and the mode of failure. The characteristic four-stage composite stress-strain behavior can be clearly seen on the load-deformation curve for both model systems. Failure occurs by the fracture of the stainless steel fibers followed by failure of the pure aluminum matrix. The method of uni-axial loading used in this work employs shoulder grips which apply direct stress only to the aluminum matrix. Fiber

tensile stresses are developed solely by the transfer of shear stress across the fiber-matrix interfacial region. It is significant to note that the aluminum/stainless steel model system exhibits synergistic performance which is commonly found in well-fabricated fiber reinforced metals. The 3-fiber model system exceeded traditional rule-of-mixtures strength predictions by approximately 9%, the 5-fiber system by 5%.

Deformation studies have been carried out through the use of microhardness techniques to measure strain hardening in the pure aluminum matrix. This work not only served to confirm the validity of the model system but also permitted study of the behavior of the metallic matrix under loading, that is, during shear stress transfer. A significant increase in Vicker's Hardness Number of the aluminum matrix was found near the ends of the stainless steel fibers. The hardness data support the contention that fiber tensile stress was indeed developed through the mechanism of shear stress transfer in the matrix. High values of matrix shear stress are expected near fiber ends in order to develop tensile stress in the fibrous reinforcement.

The observation of little change in matrix hardness as a function of radial distance from the fibers confirms earlier work done with commercially available, small-size metal matrix composite systems.

# REFERENCES

1. Jones, R.C., "Structural Metal Composites," *Civil Engineering*, ASCE, February, 1967, pp. 54-57.

2. Sutton, W.H., "Fiber-Reinforced Metals," *Modern Composite Materials*, edited by Broutman, L.J. and Krock, R.H., Addison-Wesley Publishing Company, Reading, Massachusetts, 1967, pp. 412-441.

3. Adsit, N.R., "Metal Matrix Fiber Strengthened Materials," GDC-ERR-AN-867, General Dynamics Convair, San Diego, California, December, 1965.

4. Wolff, E.G. and Hill, R.J., "Research on Boron Filament/Metal Matrix Composite Materials," Technical Report AFML-TR-67-140, June, 1967.

5. Price, D.E. and Wagner, H.J., "Preparation and Properties of Fiber-Reinforced Structural Materials," DMIC Memorandum 176, Battelle Memorial Institute, Columbus, Ohio, August, 1963.

6. Davis, L.W., "How Metal Matrix Composites Are Made," Paper presented at the ASTM/ASME Joint Symposium on Composites, Chicago, Illinois, November, 1966.

7. Burte, H.M., Bonanno, F.R. and Herzog, J.A., "Metal Matrix Composite Materials," *Orientation Effects in the Mechanical Behavior of Anisotropic Structural Materials*, ASTM STP 405, Am. Soc. Testing Mats., 1966, pp. 59-92.

8. Ebert, L.J., Hamilton, C.H. and Hecker, S.S., "Development of Design Criteria for Composite Materials," Technical Report AFML-TR-67-95, April, 1967.

9. Weeton, J.W. and Signorelli, R.A., "Fiber-Metal Composites," *Strengthening Mechanisms (Metals and Ceramics)*, Proceedings of the Twelfth Sagamore Army Material Research Conference, Edited by Burke, J.J., Reed, N.L. and Weiss, V., Syracuse University Press, 1966, pp. 477-530.

10. Schuster, D.M., "Single and Multi-Fiber Interactions in Discontinuously Reinforced Composites," Ph.D. Thesis, Cornell University, Ithaca, New York, February, 1967.

11. Kaarlela, W.T., Margolis, W.S. and Thornton, H.R., "Fundamental Study of Metal Matrix Composites," Paper presented to ASTM Symposium or Fiber Strengthened Metallic Composites, 1966 ASM National Metal Congress, Chicago, Illinois, November, 1966.

12. Kelly, A. and Davies, G.J., "The Principles of Fiber Reinforcement of Metals," *Metallurgical Reviews*, Vol. 10, No. 37, 1965, pp. 1-77.

13. Parikh, N.M., "Deformation and Fracture in Composite Materials," IITRI-B6037-6 (Final Report), IIT Research Institute, Chicago, Illinois, 31 March 1966.

14. Tyson, W.R. and Davies, G.J., "A Photoelastic Study of the Shear Stresses Associated with the Transfer of Stress During Fiber Reinforcement," *British Journal of Applied Physics*, Vol. 16, 1965, pp. 199-205.

15. Kelly, A. and Tyson, W.R., "Tensile Properties of Fiber-Reinforced Metals: Copper/Tungsten and Copper/Molybdenum," *Journal of Mechanics and Physics of Solids*, Vol. 13, 1965, pp. 329-350.

16. Sumner, E.V., "Development of Ultra High Strength, Low Density, Aluminum Plate Composites," HA-2263 (Final Report), Harvey Engineering Laboratories, Torrance, California, July, 1966.

17. Brandt, J.L., "Properties of Pure Aluminum," *Aluminum*, Edited by Van Horn, K.R., Vol. I, American Society for Metals, Metals Park, Ohio, 1967, pp. 1-30.

18. Parr, J.G. and Hanson, A., *An Introduction to Stainless Steel*, American Society for Metals, Metals Park, Ohio, 1966.

19. Broutman, L.J. and Krock, R.H., "Principles of Composites and Composite Reinforcement," *Modern Composite Materials*, edited by Broutman, L.J. and Krock, R.H., Addison-Wesley Publishing Company, Reading, Massachusetts, 1967, pp. 3-26.

20. MacFayden, D.J. and Jones, R.C., "Structural Aspects of Metal Matrix Composites," Research Report R67-64, Massachusetts Institute of Technology, Cambridge, Massachusetts, December, 1967.

21. Jones, R.C., "Deformation of Wire Reinforced Metal Matrix Composites," Research Report P67-10, Massachusetts Institute of Technology, Cambridge, Massachusetts, June, 1967.

22. Kelly, A., Strong Solids, Clarendon Press, Oxford, 1966.

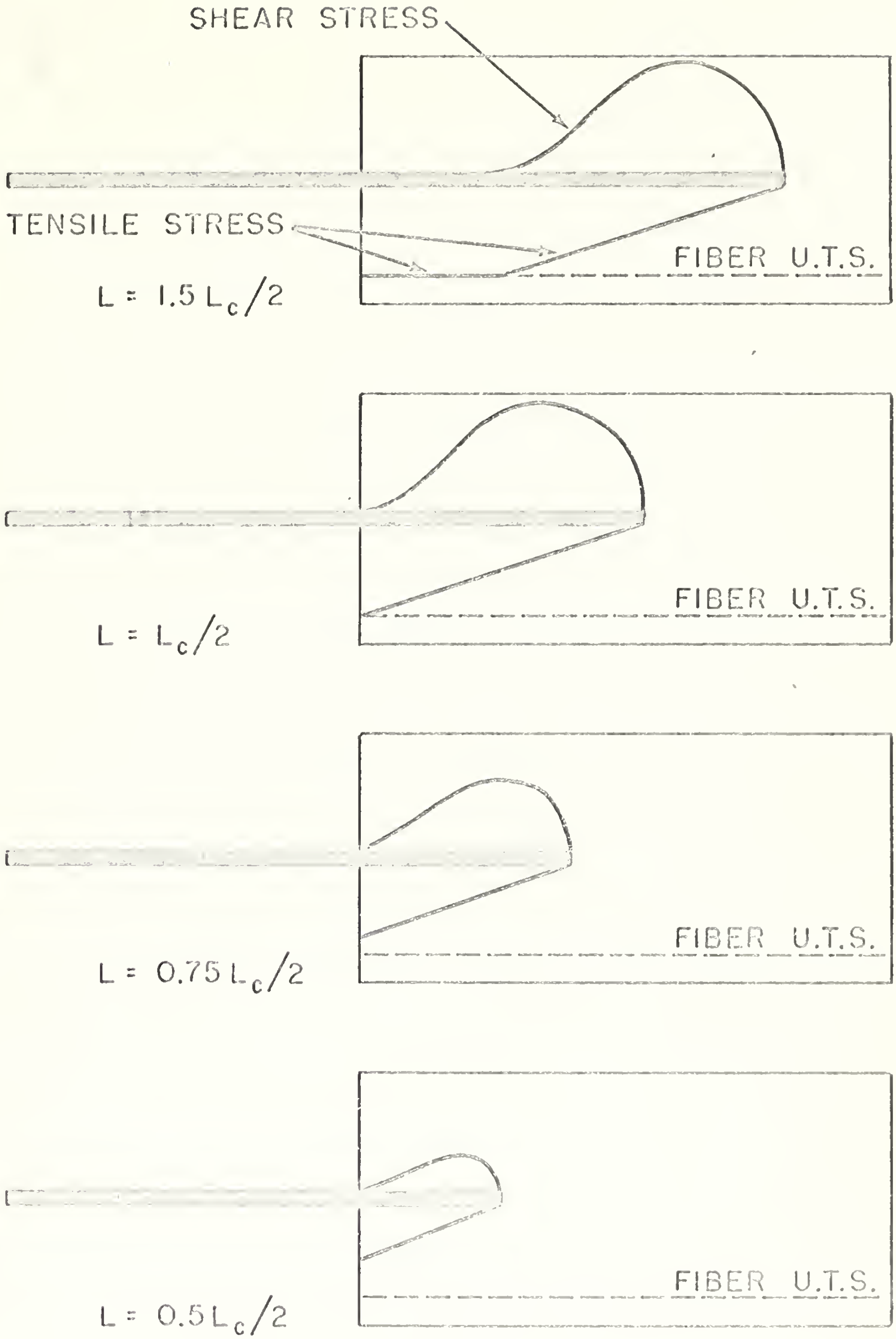

FIGURE 1. SCHEMATIC REPRESENTATION OF INTERFACIAL SHEAR STRESS AND FIBER TENSILE STRESS ALONG FIBER AXIS FOR VARIOUS DEPTHS OF FIBER EMBEDMENT

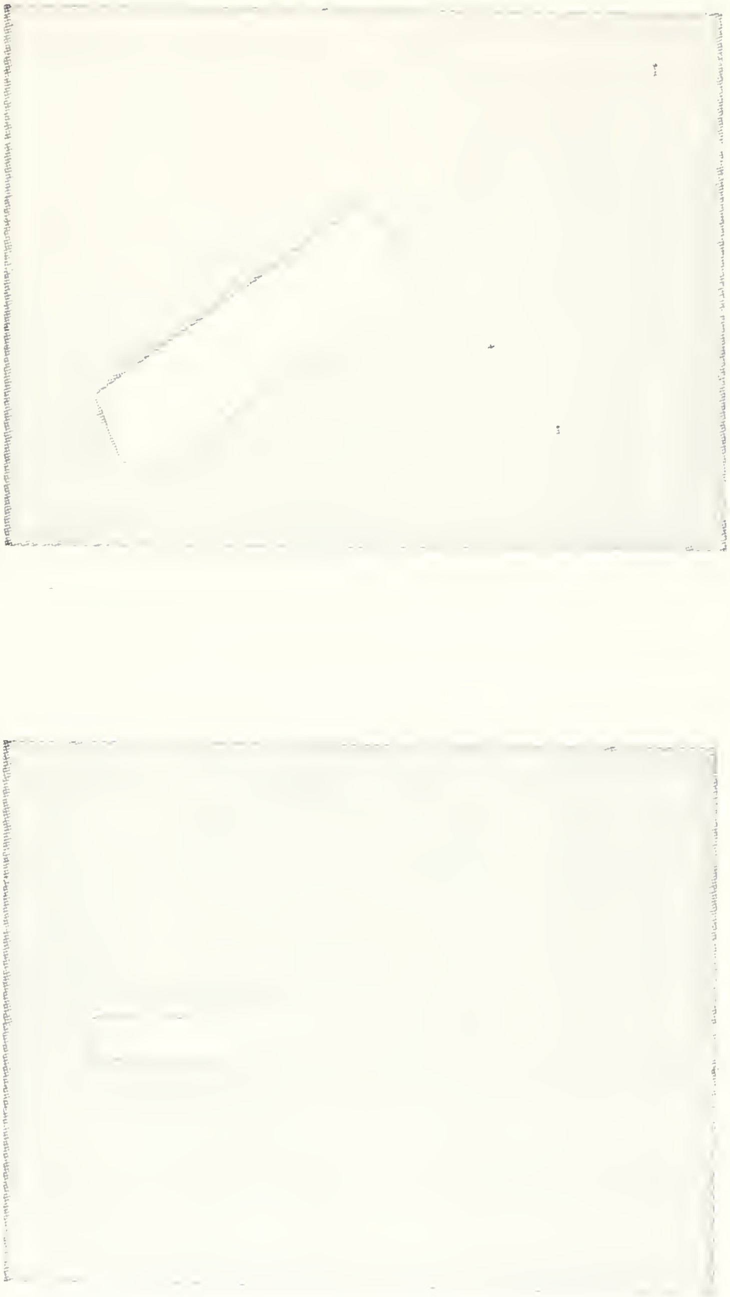

FIGURE 2. TWO VIEWS OF A PULL-OUT TEST SPECIMEN PRIOR TO TESTING

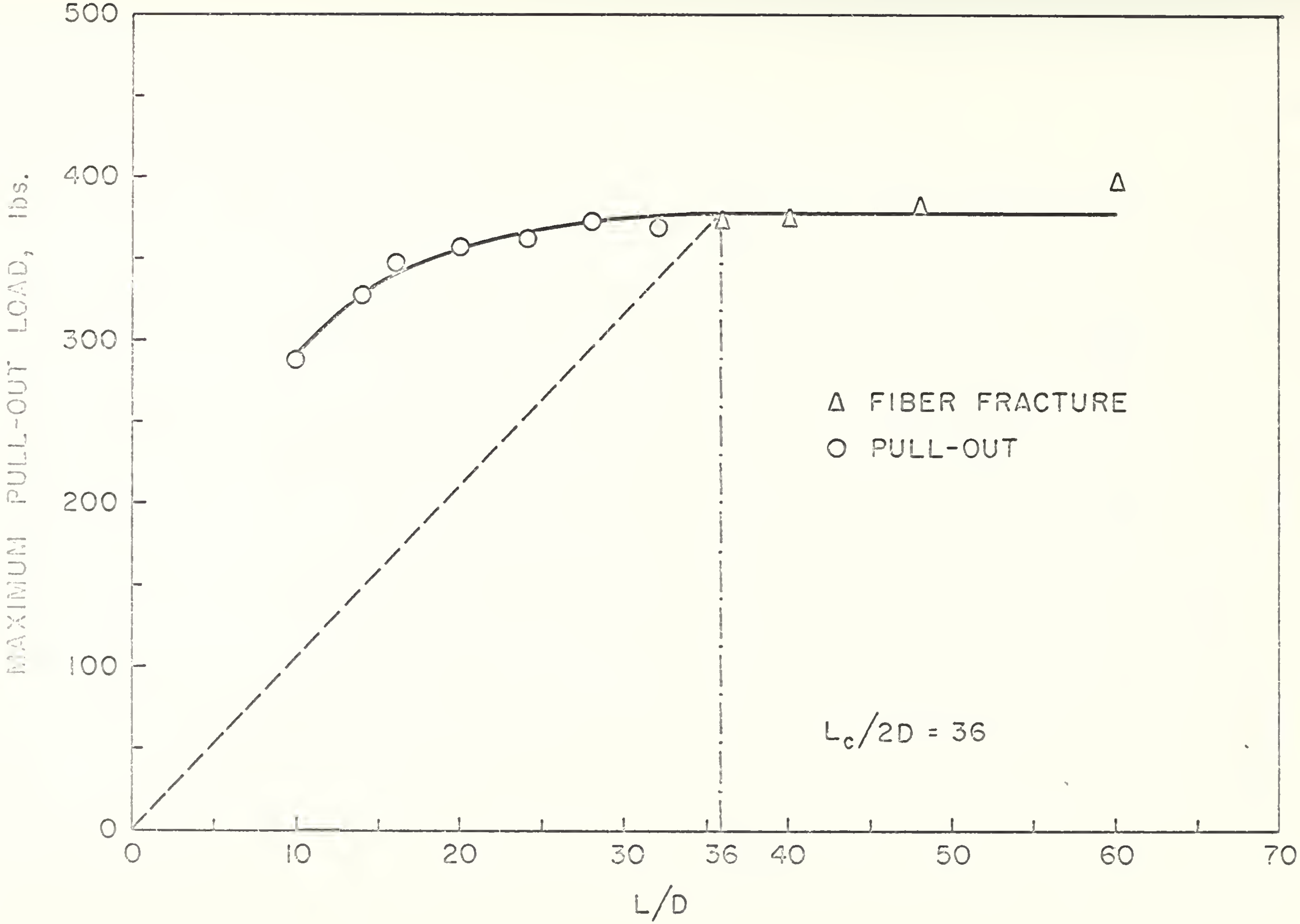

FIGURE 3. PLOT OF MAXIMUM PULL-OUT LOAD VS. LENGTH/DIAMETER RATIO

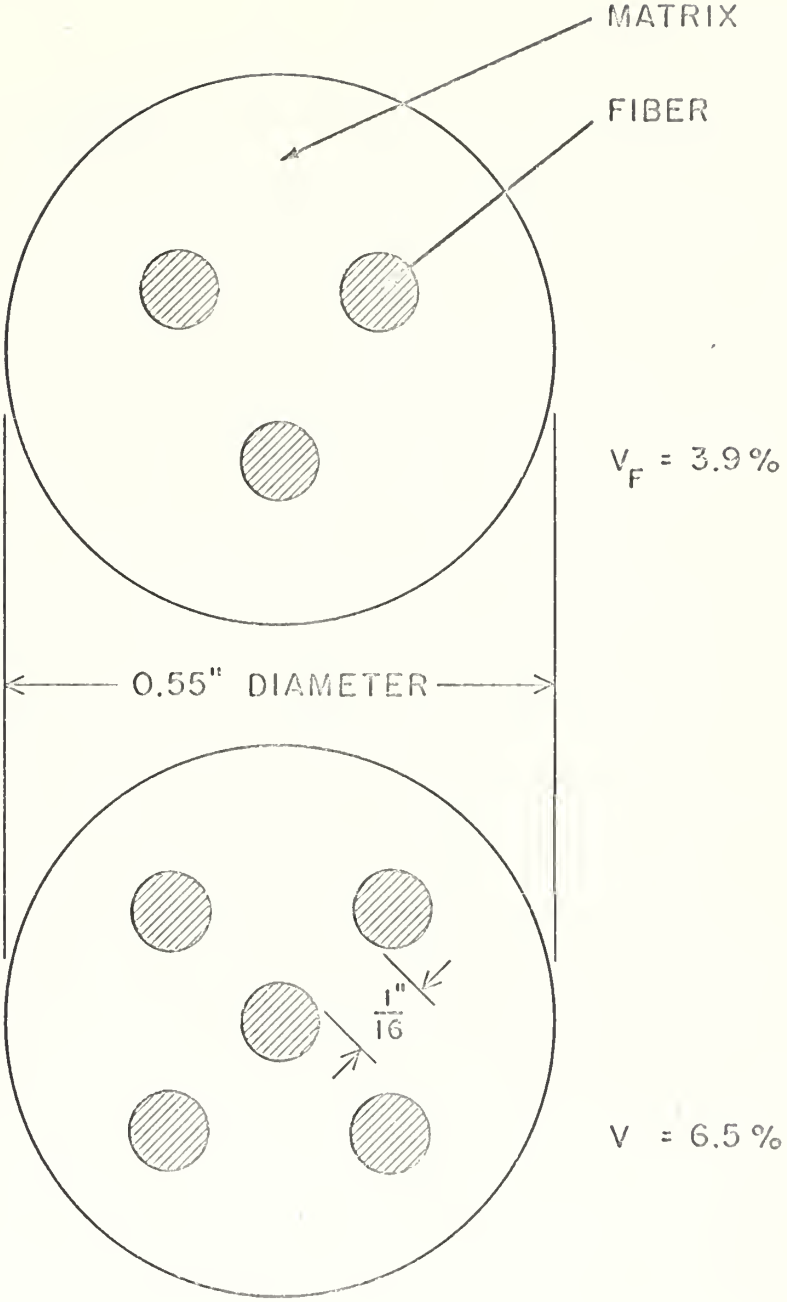

FIGURE 4. CROSS-SECTION DESIGN OF 3-FIBER AND 5-FIBER MODEL SYSTEMS

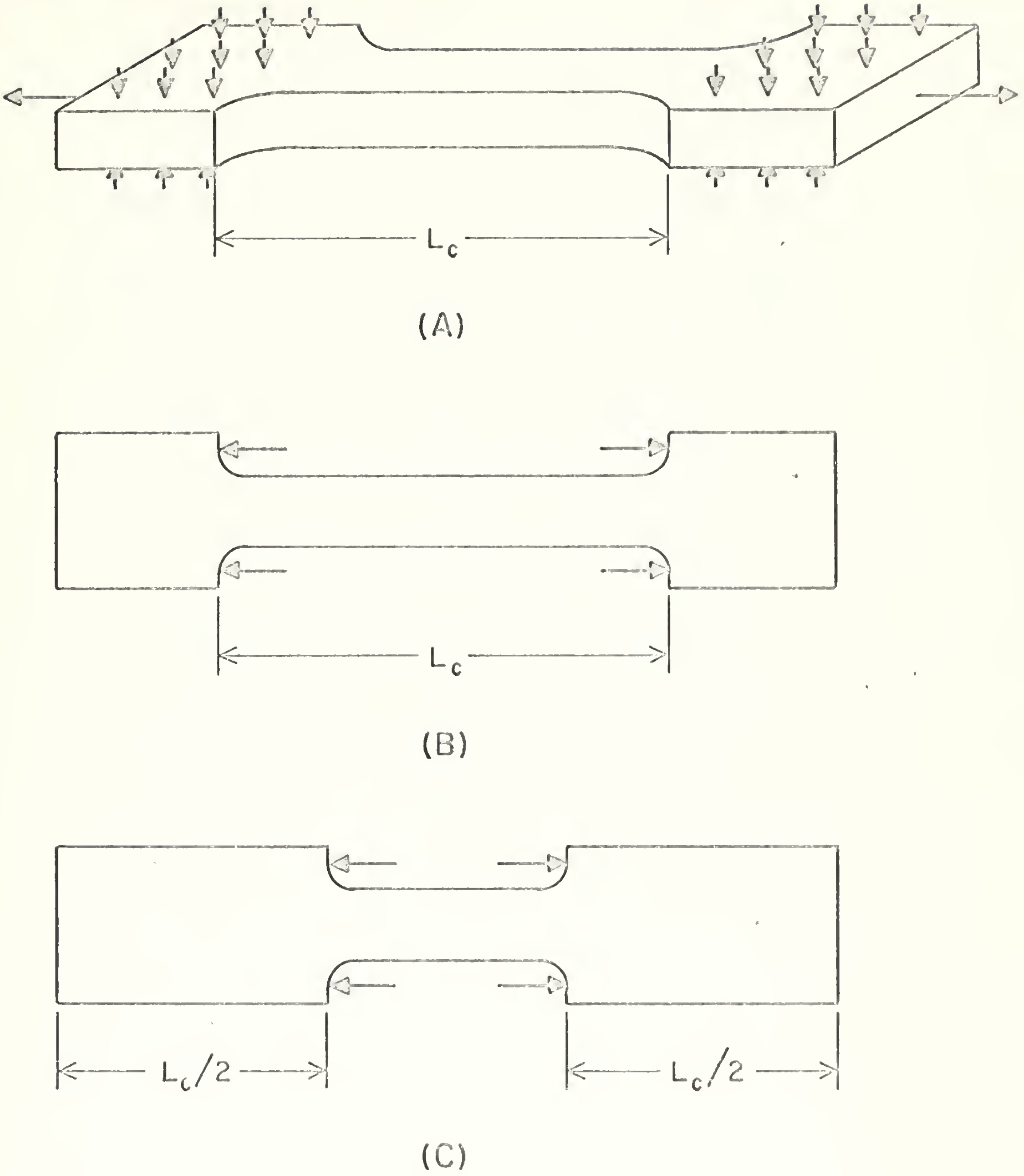

FIGURE 5. STEPS IN THE DEVELOPMENT OF THE MODEL SYSTEM DESIGN. NOTE HEAVY ARROWS INDICATING THE NATURE OF THE APPLIED LOADING.

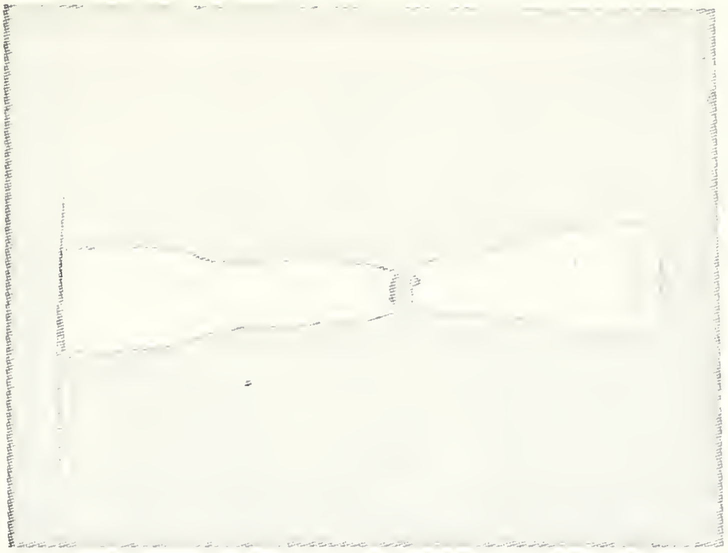

FIGURE 6. FAILURE MODE OF SEVERAL IMPROPERLY DESIGNED CONTINUOUS-FIBER MODEL SYSTEMS. SPECIMEN TESTED WITH CONVENTIONAL GRIPS SHOWN AT TOP. SPECIMENS TESTED WITH SHOULDER GRIPS SHOWN AT BOTTOM.

FIGURE 7. FINAL MODEL SYSTEM DESIGN PRIOR TO TESTING (TOP) AND AFTER FRACTURE (BOTTOM)

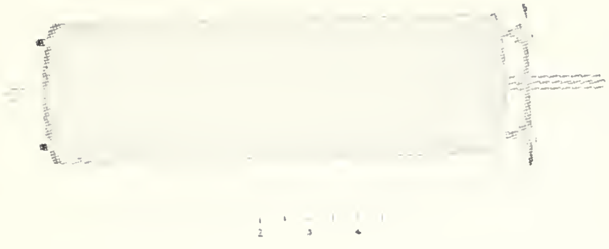

SIDE VIEW OF MOLD FOR CASTING MODEL SYSTEMS

TOP VIEW OF MOLD FOR CASTING MODEL SYSTEMS

TOP VIEW OF MOLD FOR CASTING PULL-OUT SPECIMENS

FIGURE 8. GRAPHITE MOLDS USED IN GRAVITY CASTING OPERATION

FIGURE 9. ETCHED CROSS-SECTION OF 3-FIBER MODEL SYSTEM (5X)

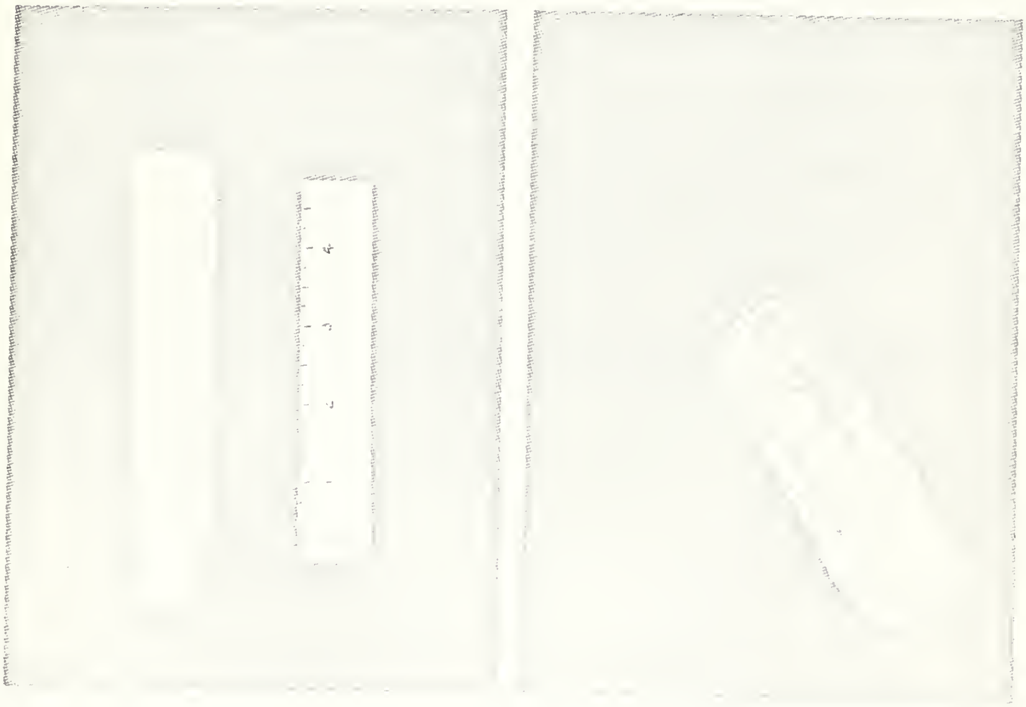

FIGURE 10. CONTINUOUS-FIBER MODEL (LEFT) AND PULL-OUT TEST SPECIMEN (RIGHT) IN AS-CAST CONDITION

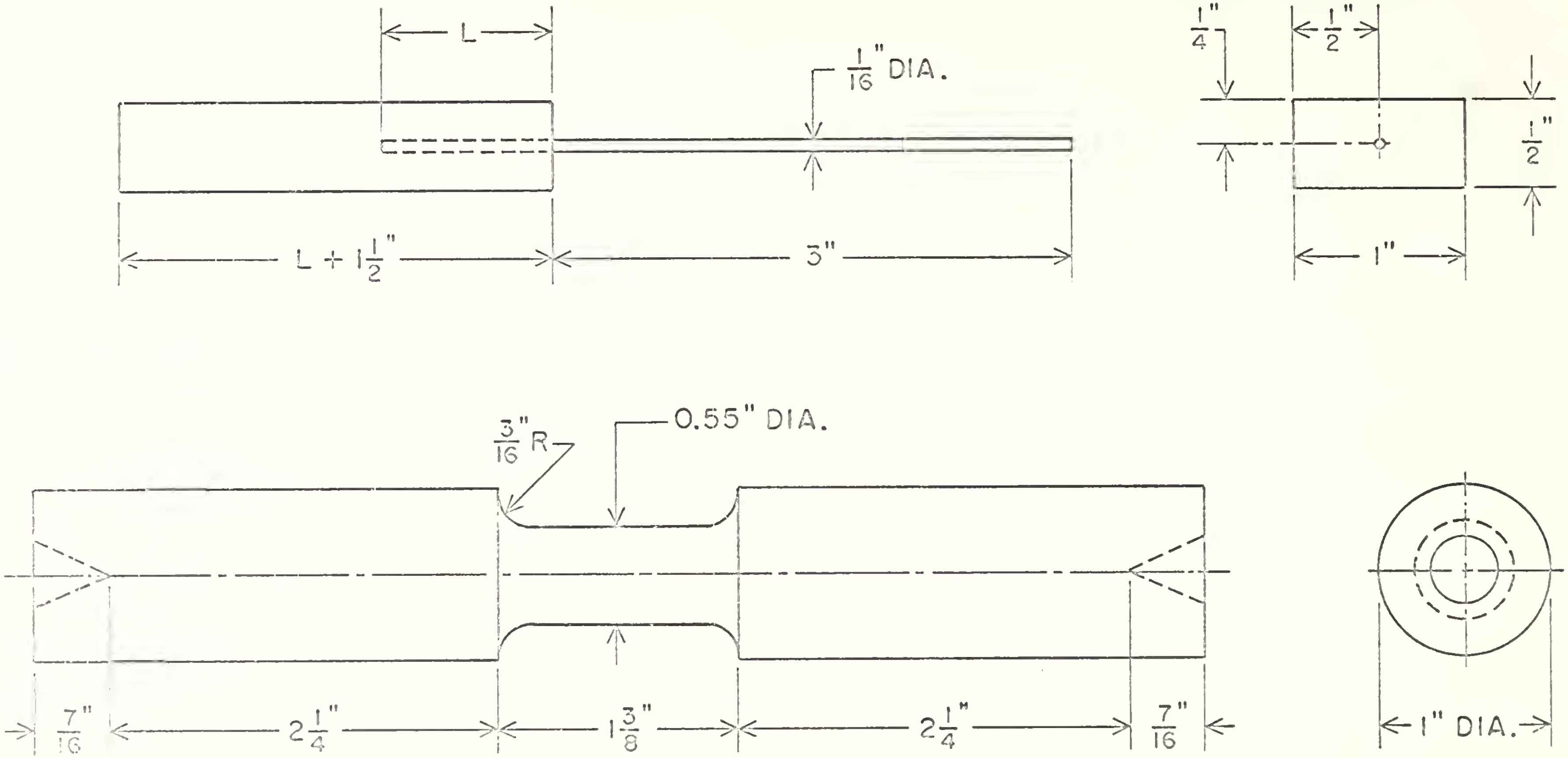

FIGURE 11. SCALED DRAWINGS OF CONTINUOUS-FIBER MODEL (BOTTOM) AND PULL-OUT TEST SPECIMEN (TOP)

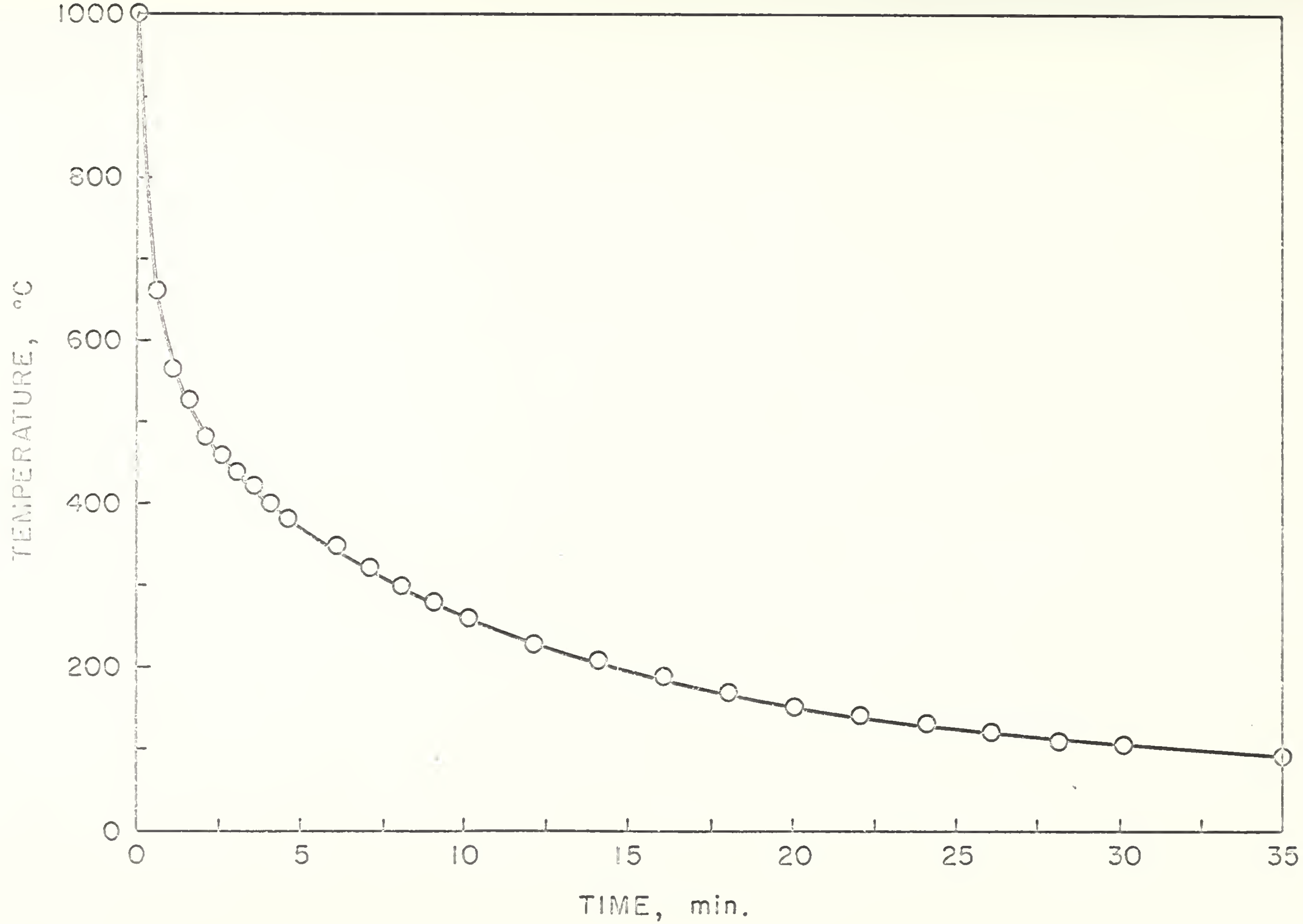

FIGURE 12. CURVE OF FIBER TEMPERATURE VS. TIME DURING THE GRAVITY CASTING OPERATION

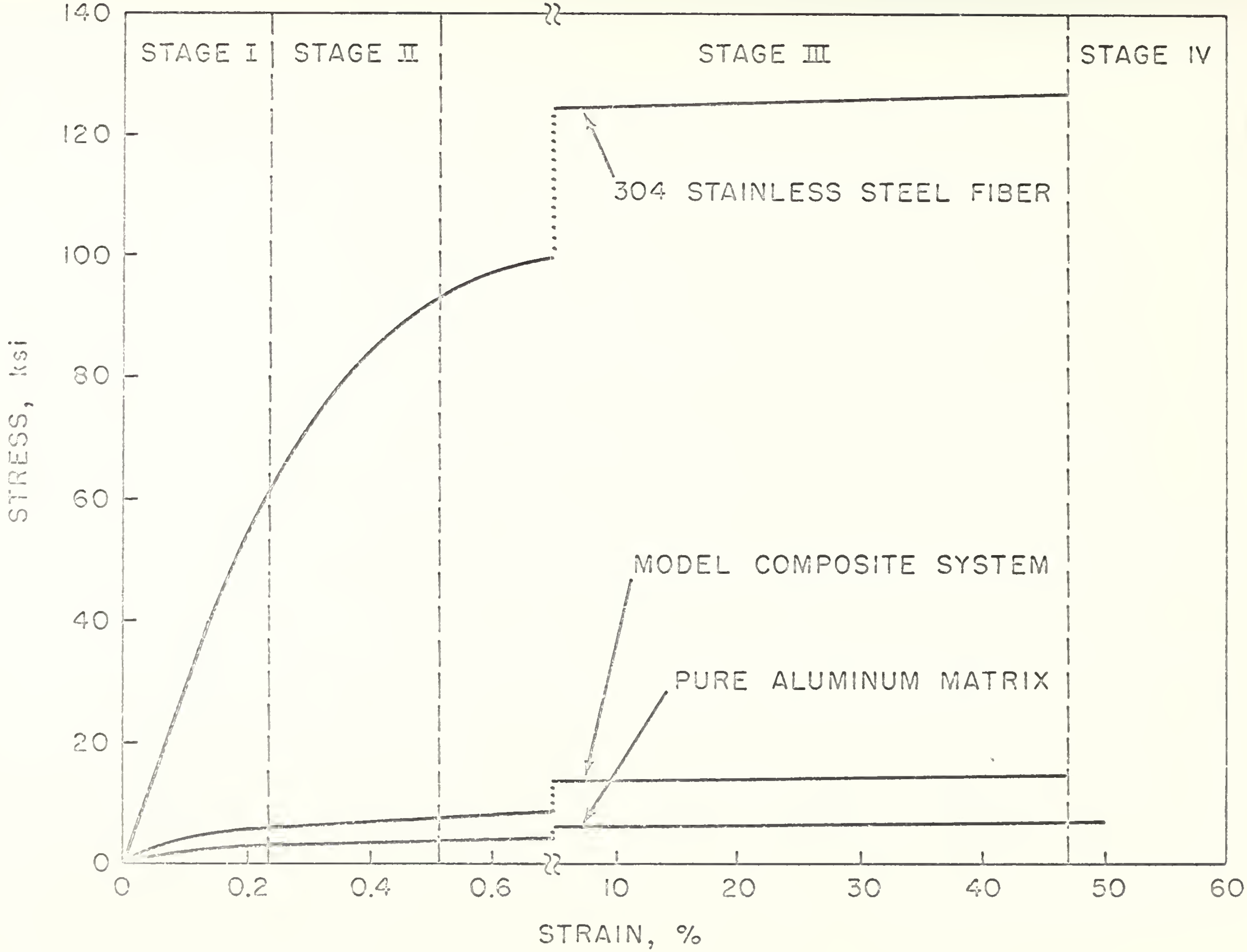

FIGURE 13. SCHEMATIC REPRESENTATION OF THE 4 STAGES OF COMPOSITE DEFORMATION

FIGURE 14. ONE END OF A CONTINUOUS-FIBER MODEL SYSTEM IN A SHOULDER GRIP

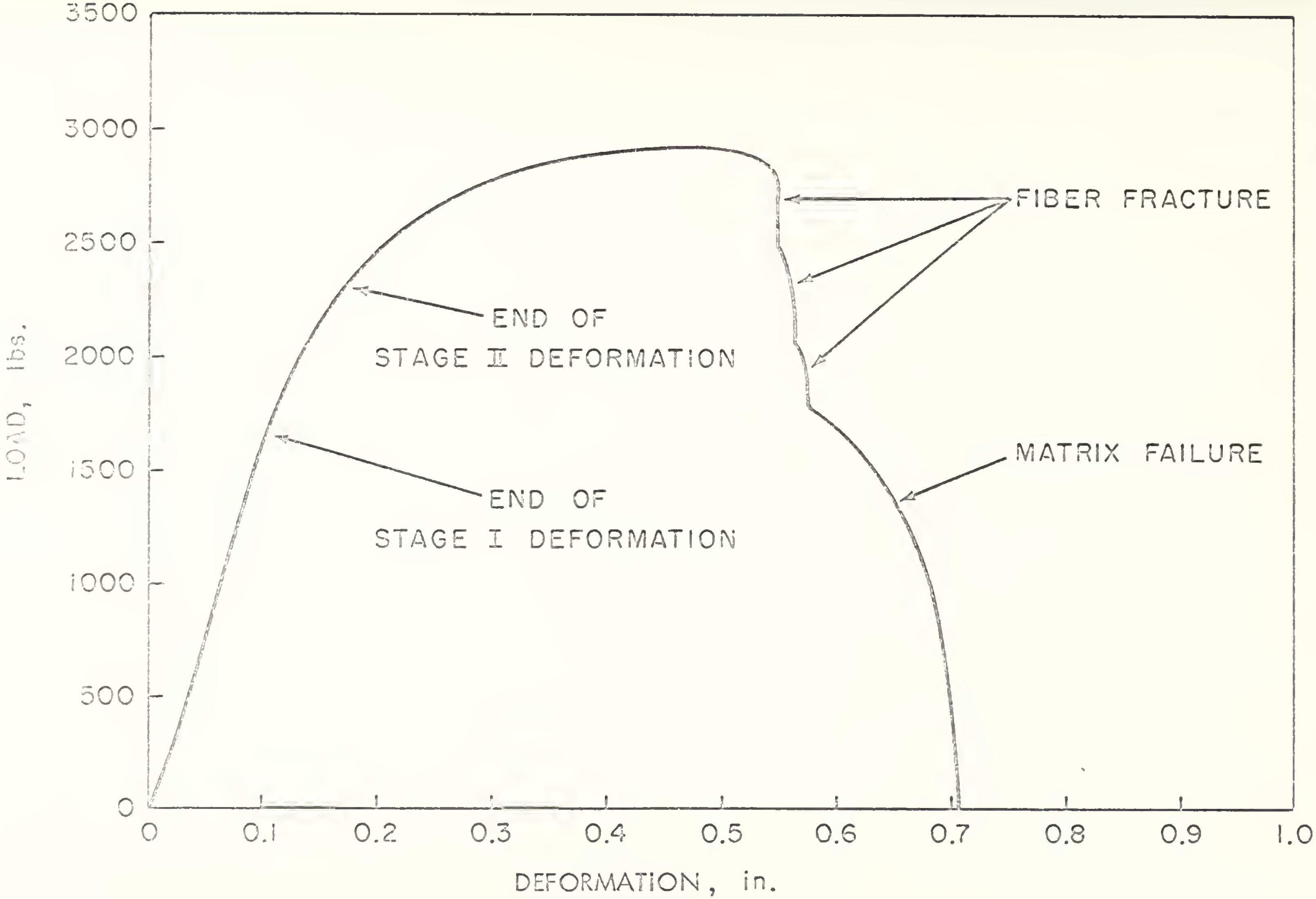

FIGURE 15. LOAD-DEFORMATION CURVE FOR 3-FIBER MODEL SYSTEM

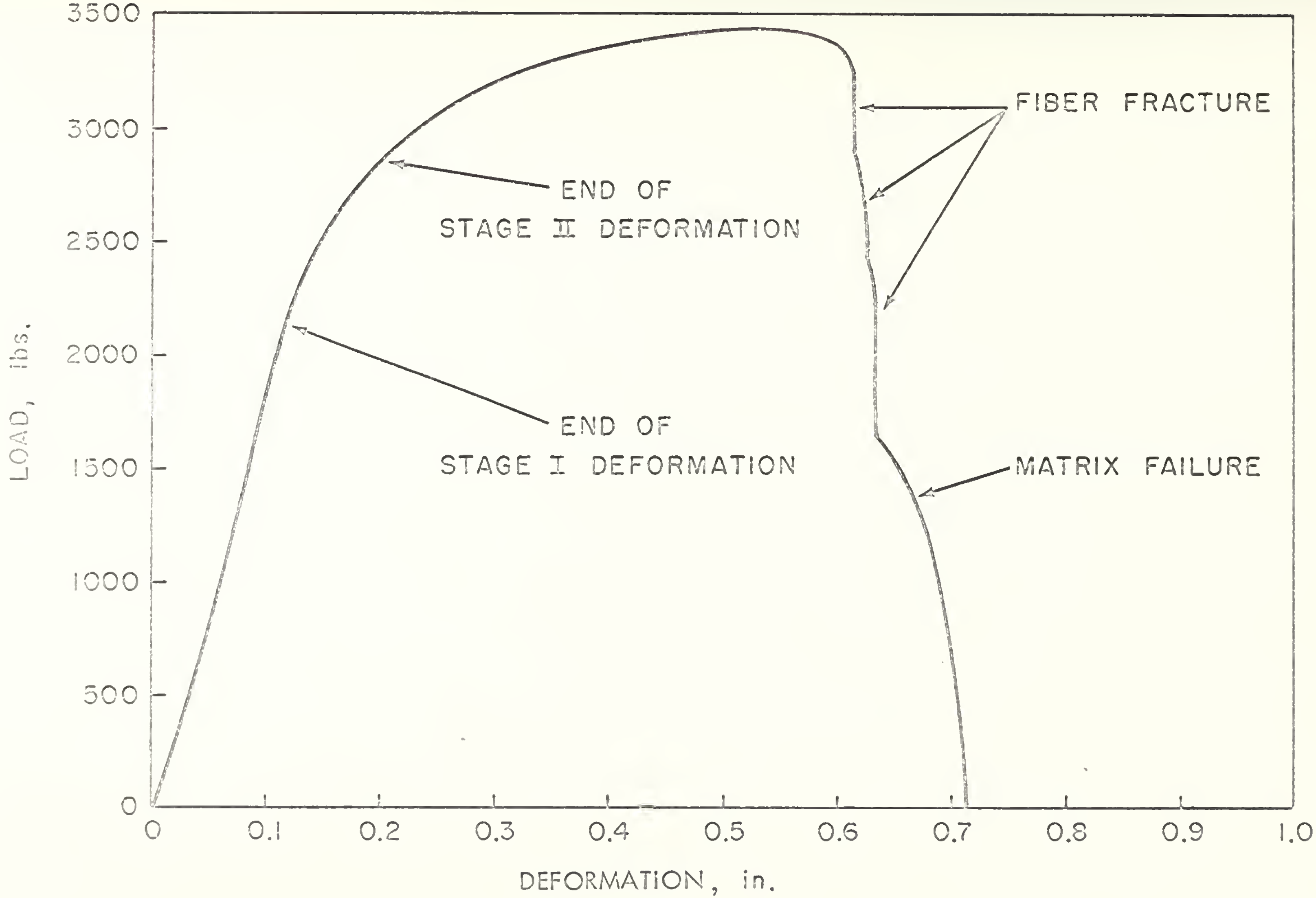

FIGURE 16. LOAD-DEFORMATION CURVE FOR 5-FIBER MODEL SYSTEM

FIGURE 17. CLUSTER OF FOUR MICROHARDNESS INDENTATIONS USED TO DETERMINE THE VICKER'S HARDNESS NUMBER (500X)

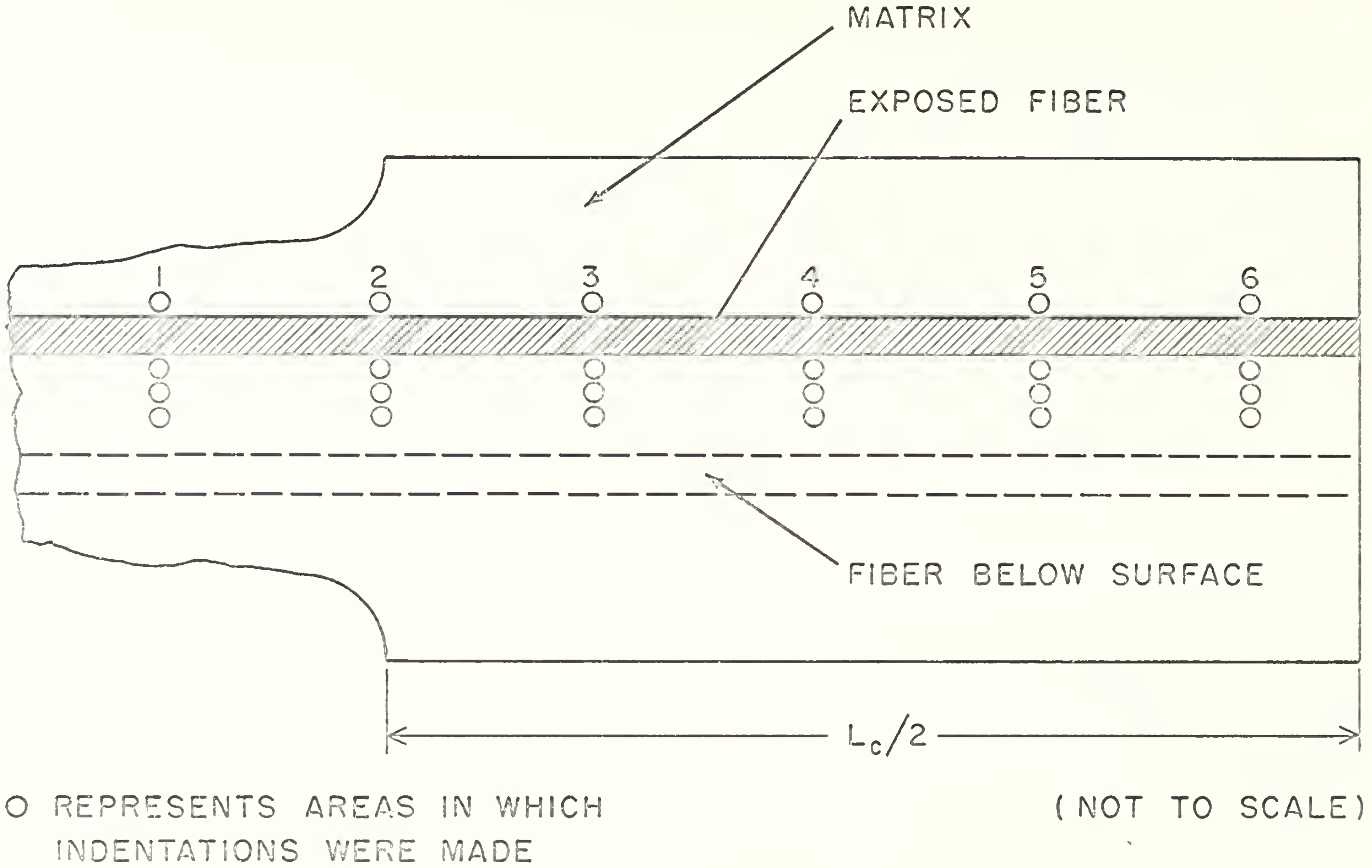

FIGURE 18. LONGITUDINAL SECTION OF FRACTURED MODEL SYSTEM SHOWING AREAS IN WHICH MICROHARDNESS INVESTIGATIONS WERE MADE

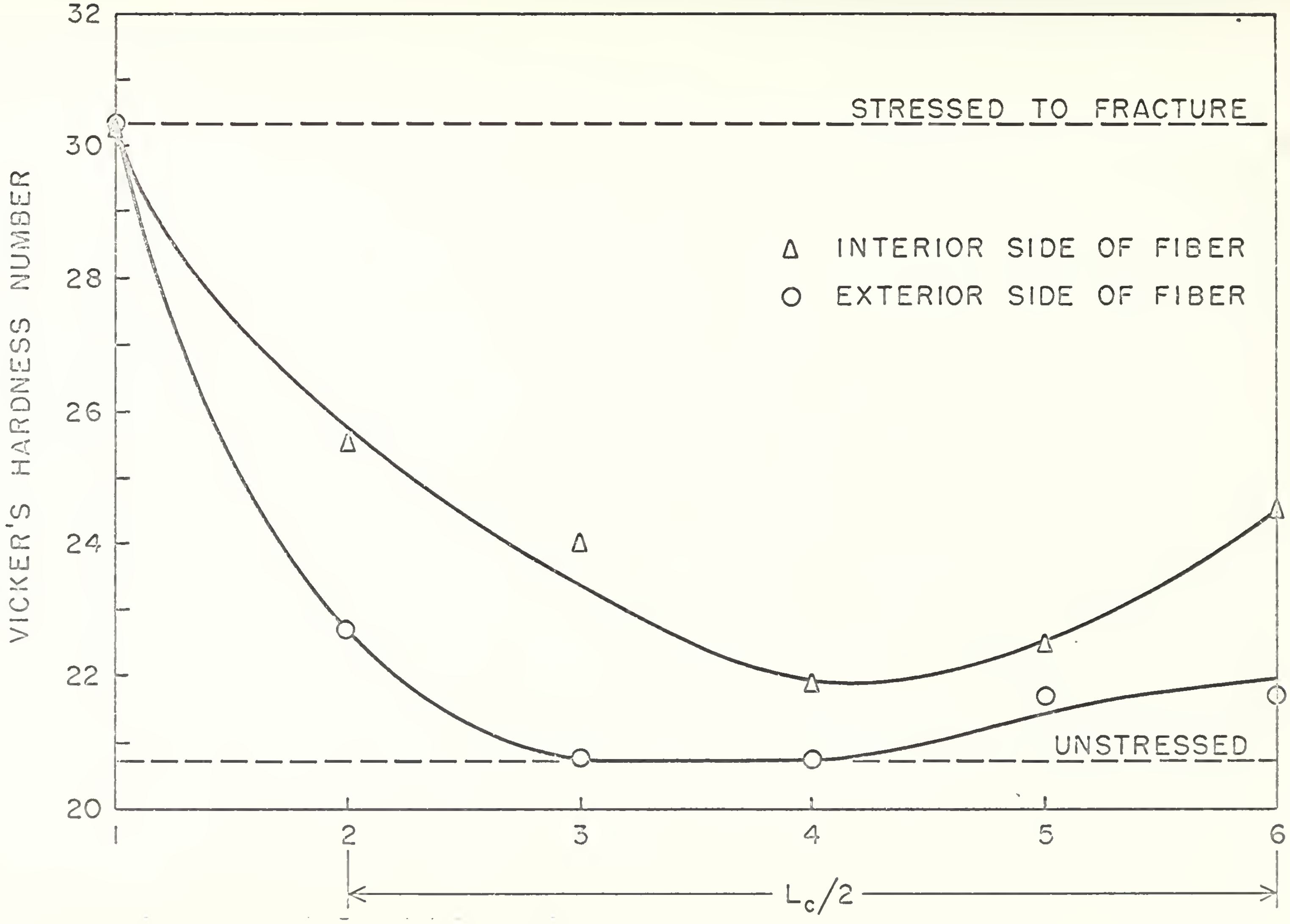

FIGURE 19. VICKER'S HARDNESS NUMBER PLOTTED AS A FUNCTION OF DISTANCE ALONG THE FIBER AXIS

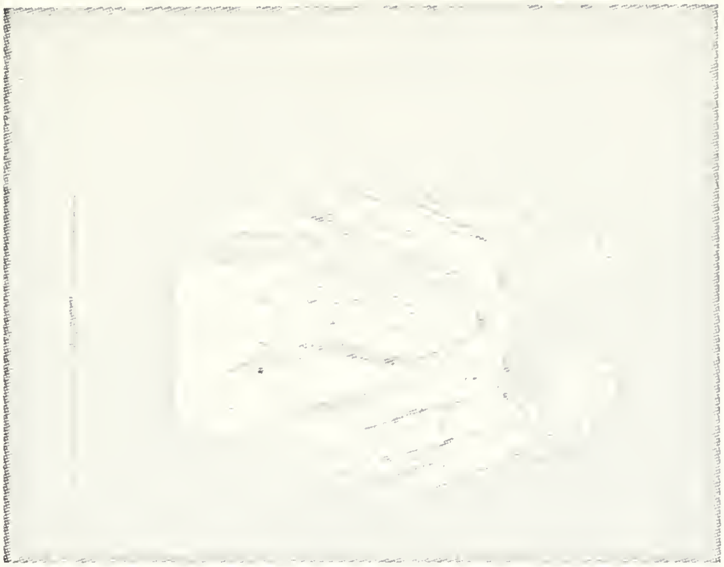

FIGURE 20. FRACTURE SURFACE OF 3-FIBER MODEL SYSTEM VIEWED AT 45° (TOP) AND 90° (BOTTOM)(5X)

FIGURE 21. FRACTURE SURFACE OF 5-FIBER MODEL SYSTEM VIEWED AT 45° (TOP) AND 90° (BOTTOM)(5X)

FIGURE 22. SCANNING ELECTRON MICROGRAPH OF FRACTURE SURFACES OF A COMMERCIAL 2024 ALUMINUM/NS355 STAINLESS STEEL COMPOSITE (.006" FIBERS). TOP MICROGRAPH VIEWED AT 45°; BOTTOM MICROGRAPH SHOWS "CUP AND CONE" FRACTURE SURFACE OF A SINGLE FIBER.

# Appendix

# LIST OF FIGURES

Figure — Page

1. Schematic Representation of Interfacial Shear Stress and Fiber Tensile Stress Along Fiber Axis for Various Depths of Fiber Embedment........ 43
2. Two Views of a Pull-Out Test Specimen Prior to Testing........ 44
3. Plot of a Maximum Pull-Out Load vs. Length/Diameter Ratio........ 45
4. Cross-Section Design of 3-Fiber and 5-Fiber Model Systems........ 46
5. Steps in the Development of the Model System Design........ 47
6. Failure Mode of Several Improperly Designed Continuous-Fiber Model Systems........ 48
7. Final Model System Design Prior to Testing and After Fracture........ 49
8. Graphite Molds Used in Gravity Casting Operation........ 50
9. Etched Cross-Section of 3-Fiber Model System.. 51
10. Continuous-Fiber Model and Pull-Out Test Specimen in the As-Cast Condition........ 51
11. Scaled Drawings of Continuous-Fiber Model and Pull-Out Test Specimen........ 52
12. Curve of Fiber Temperature vs. Time During the Gravity Casting Operation........ 53
13. Schematic Representation of the Four Stages of Composite Deformation........ 54
14. One End of a Continuous-Fiber Model System in a Shoulder Grip........ 55

Figure Page

15. Load-Deformation Curve for the 3-Fiber Model System........................ 56

16. Load-Deformation Curve for the 5-Fiber Model System........................ 57

17. Cluster of Four Microhardness Indentations Used to Determine the Vicker's Hardness Number........................................ 58

18. Longitudinal Section of Fractured Model System Showing Areas in which Microhardness Investigations Were Made........... 59

19. Vicker's Hardness Number Plotted as a Function of Distance Along Fiber Axis....... 60

20. Fracture Surface of 3-Fiber Model System.... 61

21. Fracture Surface of 5-Fiber Model System.... 62

22. Scanning Electron Micrographs of Fracture Surfaces of a Commercial 2024 Aluminum/NS355 Stainless Steel Composite............. 63

thesF97
Deformation and fracture of a metal matr
3 2768 001 90707 4
DUDLEY KNOX LIBRARY